

LTP is accompanied by an enhanced local excitability of pyramidal neuron dendrites

Andreas Frick^{1,2}, Jeffrey Magee^{2,3} & Daniel Johnston^{1,2}

The propagation and integration of signals in the dendrites of pyramidal neurons is regulated, in part, by the distribution and biophysical properties of voltage-gated ion channels. It is thus possible that any modification of these channels in a specific part of the dendritic tree might locally alter these signaling processes. Using dendritic and somatic whole-cell recordings, combined with calcium imaging in rat hippocampal slices, we found that the induction of long-term potentiation (LTP) was accompanied by a local increase in dendritic excitability that was dependent on the activation of NMDA receptors. These changes favored the back-propagation of action potentials into this dendritic region with a subsequent boost in the Ca^{2+} influx. Dendritic cell-attached patch recordings revealed a hyperpolarized shift in the inactivation curve of transient, A-type K^+ currents that can account for the enhanced excitability. These results suggest an important mechanism associated with LTP for shaping signal processing and controlling dendritic function.

Action potentials initiated near the soma actively back-propagate into the dendritic tree of pyramidal neurons^{1–3}, thereby providing strong postsynaptic depolarization and Ca^{2+} influx^{4–7}. The amplitude of these back-propagating action potentials (b-APs), however, attenuates with distance from the soma^{3,6,8}. In CA1 pyramidal neurons, this decrement is largely due to a steep increase in the density of a transient, outward current toward the distal dendrites⁹. These A-type K^+ channels not only suppress b-APs, but also reduce excitatory synaptic potentials (EPSPs)¹⁰ and raise the threshold for local AP initiation⁹. Any modulation of A-type K^+ channels will therefore impact overall dendritic excitability¹¹. The transient nature of these channels, for example, allows for an amplification of b-APs when appropriately timed with synaptic input¹², a process that has been implicated in certain Hebbian forms of plasticity^{12,13}. In addition to voltage, the properties of A-type K^+ channels can be modified by a change in phosphorylation state or oxidative modulation. Activation of protein kinase A (PKA), protein kinase C (PKC) and mitogen-activated protein kinase (MAPK) produces a depolarizing shift in the activation curve of A-type K^+ channels^{8,14}, whereas modulation by arachidonic acid causes a reduction in the current and a hyperpolarized shift in the inactivation curve^{10,15}. These mechanisms have been shown to increase the amplitude of b-APs^{14,16}, and they can be accomplished through the activation of several neurotransmitter systems, including the glutamatergic, dopaminergic, adrenergic and cholinergic systems^{14,17}. Furthermore, the induction of LTP leads to a transient or persistent activation of many of the same protein kinases and modulators¹⁸.

LTP is an activity-dependent, prolonged increase in the strength of synaptic connections and is thought to be a component mechanism

underlying aspects of learning and memory¹⁹. In addition to changes in synaptic strength, the propensity of a postsynaptic neuron to fire APs in response to a given EPSP is enhanced after LTP induction, suggesting a higher efficiency of EPSP-to-spike coupling. This phenomenon is known as EPSP-spike (E-S) potentiation²⁰. Most studies of plasticity have focused on changes in synaptic strength, but other potential candidates for activity-dependent changes in neuronal function include the wide array of voltage-gated Na^+ , K^+ and Ca^{2+} ion channels expressed in the dendrites of these neurons^{11,21–25}. The density and distribution of these channels largely governs synaptic integration and neuronal excitability^{26,27}. This suggests that if activity could selectively modulate the expression or the activation/inactivation state of these dendritic channels, then the integrative properties of a neuron could be markedly altered.

In this study, we tested whether a modulation of the transient K^+ current, I_A , was associated with synaptic potentiation and could be detected locally in the dendrite. Consequences of a down-regulation of I_A would be a dynamic modification of dendritic signaling, including enhanced back-propagation of action potentials and the associated Ca^{2+} influx and improved transfer of synaptic potentials and thereby coupling to spike initiation. We used whole-cell recordings and Ca^{2+} imaging in dendrites to measure the amplitude of b-APs and of the concomitant Ca^{2+} signals before and after inducing LTP. We found a persistent and local increase in the b-AP amplitude and the associated Ca^{2+} signals in the dendritic region where the synapses were stimulated. Dendritic, cell-attached recordings revealed a hyperpolarized shift in the inactivation curve of I_A with LTP induction. These results strongly support the idea of activity-dependent, local alterations in neuronal function.

¹Division of Neuroscience, Baylor College of Medicine, One Baylor Plaza, Houston, Texas 77030, USA. ²Marine Biological Laboratory, Woods Hole, Massachusetts 02543, USA. ³Neuroscience Center, LSU Health Science Center, 2020 Gravier Street, New Orleans, Louisiana 70112, USA. Correspondence should be addressed to D.J.J. (dan@mossy.bcm.tmc.edu).

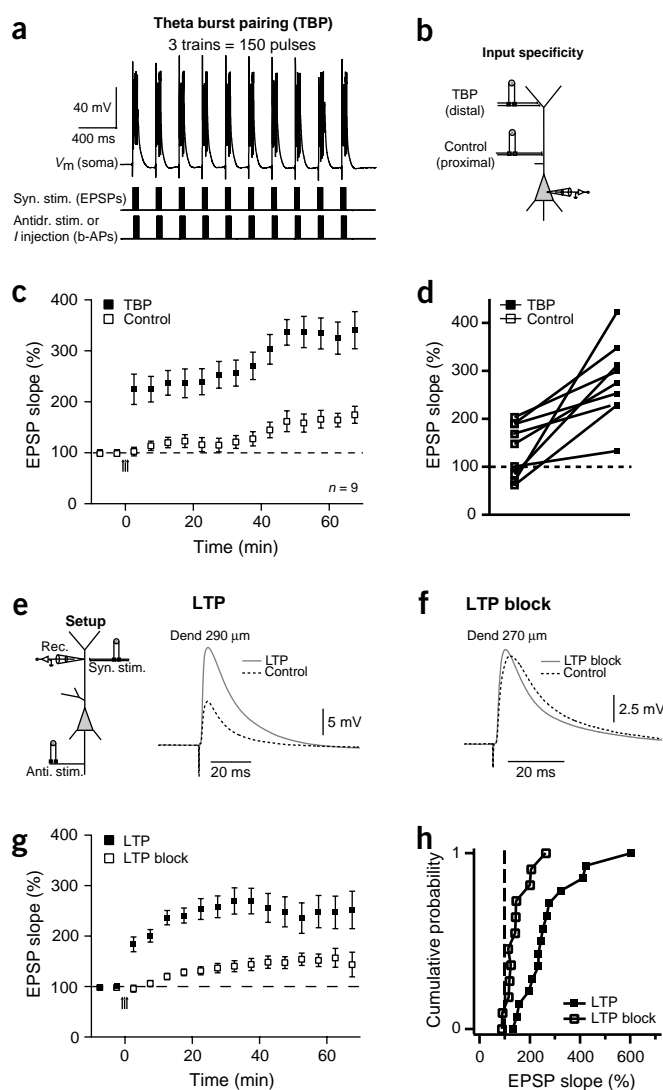


Figure 1 Theta-burst pairing (TBP) induced strong and pathway-specific LTP. **(a–d)** Somatic recordings. **(a)** A theta-burst pairing (TBP) protocol of synaptic and antidromic stimulation was used to induce LTP. The upper trace illustrates a representative response to a train of TBP. **(b)** Experimental setup to determine pathway specificity. **(c)** Time course and magnitude of potentiation. TBP resulted in strong LTP in the tetanized (TBP), but not in the control pathway (control). **(d)** Plot showing the difference in the potentiation for the TBP versus the control pathway for each experiment (30–35 min after TBP). **(e–h)** Dendritic recordings. **(e)** Experimental setup: responses were recorded in the distal dendrite close to the stimulating electrode. Representative recording at a distance of 290 μm from the soma shows strong potentiation of the EPSP 30 min after application of the TBP protocol. **(f)** Antagonists of the NMDA receptor (50 μM D,L-APV and 10 μM MK-801) suppressed the TBP-induced LTP. Representative EPSP responses are shown before (control) and after TBP in the presence of antagonists (LTP block). **(g)** Time course and magnitude of potentiation evoked by TBP (LTP), as compared to TBP in the presence of NMDA receptor antagonists (LTP block). **(h)** Cumulative probability plot summarizes the data from **g**. Each point represents the magnitude of change relative to baseline for any given experiment, typically 30–35 min after TBP (probability of 50% long-term increase in EPSP with TBP, 93%; with TBP in the presence of antagonists, 33%).

quency (5 Hz, theta-burst pairing protocol, TBP) (Fig. 1a). This protocol consisted of three trains of ten bursts repeated at 0.1 Hz, with each burst composed of five EPSPs paired with five b-APs at 100 Hz. The b-APs were timed so that the peaks of the APs were coincident with the approximate peaks of the EPSPs, as measured in the soma.

The experimental configuration is shown in Figure 1b. A distal pathway ($237 \pm 30 \mu\text{m}$, mean \pm s.d., from the soma) served as the test pathway and was tetanized according to the described TBP protocol. A second non-tetanized, proximal pathway ($52 \pm 16 \mu\text{m}$) served as the control. In each neuron, strong LTP was induced in the tetanized pathway and little or no potentiation in the control pathway (Fig. 1c,d); analysis of grouped data showed a significant difference between the two pathways (EPSP slope, 277% (tetanized) vs. 135% (control), $n = 9$, $P < 0.005$, 30–35 min after LTP induction). This has been interpreted as the input-specific response resulting from the induction protocol. Notably, the synaptic inputs from the control pathway showed a small, slowly developing potentiation. Although this form of heterosynaptic plasticity has been observed in other studies using the TBP induction paradigm^{13,28}, the mechanisms are not known.

Dendritic changes in EPSP amplitude after LTP

We also measured changes in the synaptic responses induced by the TBP protocol using dendritic recordings close to the site of the stimulation ($259 \pm 28 \mu\text{m}$ from soma, Fig. 1e–h). For this TBP protocol, EPSPs and b-APs were timed so that the peaks of the b-APs were coincident with the peaks of the EPSPs, as measured in the dendrite (Fig. 1e, one representative example shown at right). Summary data from 15 experiments are also shown (Fig. 1g,h). As expected, LTP induction led to a strong increase in the slope of the EPSPs ($274 \pm 32\%$, 30–35 min after TBP), accompanied by a modest increase in input resistance ($111 \pm 4\%$, $n = 10$, $P < 0.05$). To determine whether LTP induction was dependent on the activation of NMDA receptors, we performed additional experiments in which we added the specific NMDA receptor antagonists D,L-APV (50 μM) and MK-801 (10 μM) to the bath before applying the TBP protocol. Under those conditions, EPSP potentiation was prevented or significantly reduced as compared to the drug-free condition ($146 \pm 15\%$, $n = 12$, vs. $274 \pm 32\%$, $n = 15$; $P < 0.005$; Fig. 1f–h).

RESULTS

We examined the effects of LTP induction on dendritic excitability using a combination of dendritic or somatic whole-cell recordings and calcium imaging in CA1 neurons from adult rats. Pyramidal neurons were filled with the Ca^{2+} indicator bis-fura-2 and changes in $[\text{Ca}^{2+}]_i$ ($\Delta F/F$) were measured using a charge-coupled device (CCD) camera. EPSPs were evoked at a distance of 200–300 μm from the soma by extracellular stimulation in stratum radiatum at close proximity ($< 25 \mu\text{m}$) to the dendrite. The amplitudes of the EPSPs were 2–6 mV (measured at the soma) or 4–9 mV (measured at the dendrite). b-APs were elicited by brief current injections to the soma or by antidromic stimulation, and the resulting changes in voltage or $[\text{Ca}^{2+}]_i$ were examined in the apical dendrites. Dendritic, cell-attached recordings were performed to study the effect of LTP induction on the activation/inactivation properties of I_A . All experiments were conducted at near-physiological temperatures (32–36 $^{\circ}\text{C}$).

LTP induction and input specificity

To determine the specificity and magnitude of the LTP response, potentiation of synaptic inputs was measured in both a test and a control pathway. LTP was induced using a protocol consisting of subthreshold synaptic stimulation paired with b-APs at theta fre-

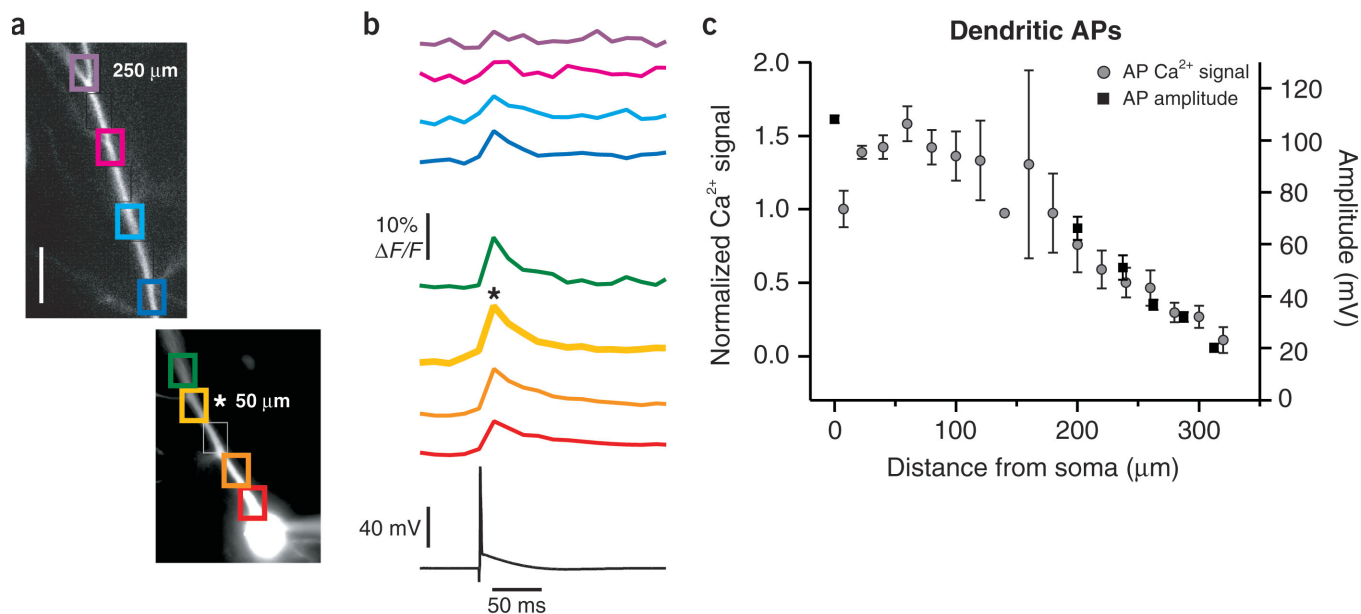


Figure 2 Profile of b-AP-induced Ca²⁺ signals along the main apical dendrite. **(a)** Fluorescence image of a CA1 pyramidal neuron filled with bis-fura-2 via a somatic recording pipette. Scale bar, 20 μm. **(b)** A single b-AP (lower trace) was induced by current injection into the soma, and the influx of Ca²⁺ from that b-AP was measured as % ΔF/F along the apical trunk (upper traces). Representative Ca²⁺ traces are shown (corresponding to colored boxes in **a**). The Ca²⁺ influx peaked in the proximal region (~50 μm from soma, *) and then gradually decreased with distance. **(c)** Summary of this analysis for 15 neurons. The peak values of the Ca²⁺ responses (circles) from b-APs are plotted as function of distance from the soma. For comparison, the amplitude of APs (squares), obtained with somatic ($n = 15$) or dendritic recordings ($n = 58$), was plotted over the same distance along the dendrite.

Ca²⁺ signals from b-APs

Previous studies have shown that b-APs elicit rises in $[Ca^{2+}]_i$ in the dendrites through activation of voltage-gated Ca²⁺ channels^{4,5,7,29}. In the present experiments, Ca²⁺ influx from b-APs was measured along the main apical dendrite as a function of distance from the soma. The results from one experiment are shown (Fig. 2a,b). The changes in $[Ca^{2+}]_i$ from a single b-AP were quantified at 10–20 μm intervals over a region of about 250 μm along the main trunk. The Ca²⁺ signals for some of these locations (see colored boxes in Fig. 2a) and the electrical recording of the b-AP measured in the soma (lower trace), are shown in Figure 2b. The rise in $[Ca^{2+}]_i$ was largest in the proximal part of the dendrite approximately 50 μm from the soma (Fig. 2c, $50 \pm 22 \mu\text{m}$, $165 \pm 53\%$, $n = 15$). Beyond that region of the dendrite, the Ca²⁺ signals became progressively smaller with increasing distance from the soma. The results from 15 similar experiments are shown in Figure 2c (circles). From previous studies^{8,12,30} and also shown here (Fig. 2c), the amplitude of the b-AP, on average, would be expected to decline by about 60% within the first 250 μm of the main apical dendrite (soma, $n = 15$, dendrite, $n = 58$), whereas the density of I_A would be expected to increase by 4- to 5-fold over the same region⁹. Since the decrease in b-AP amplitude is predominantly caused by a high density of I_A in the distal dendrites of these neurons^{7,9}, it is reasonable to assume that any mechanism that downregulates I_A would result in larger amplitudes of b-APs. Potential modulators of I_A properties, such as PKA, PKC, MAPK and arachidonic acid¹⁸, are known to be activated by the induction of LTP. We therefore hypothesized that LTP induction would be accompanied by a down-regulation of I_A and a subsequent increase in the amplitude of the b-APs in the region where LTP has occurred. The following experiments were designed to test various elements of this hypothesis.

Changes in Ca²⁺ signals after LTP

The fact that voltage-gated Ca²⁺ channels are sensitive indicators of the amplitude of b-APs^{4,5,7,12} led us to predict that a modulation of the b-AP amplitude following LTP induction would be detectable as a change in the associated Ca²⁺ signals. We therefore measured changes in Ca²⁺ signals from b-APs before and after the induction of LTP within the distal dendritic region where the synaptic inputs were stimulated, as well as in the soma and the proximal dendrites. This approach has the advantage that it obviates the need to record at the exact location where LTP is induced in the dendrite to detect changes in b-AP amplitude. Accordingly, whole-cell recordings were performed at the soma or at the dendrite, and the cells were equilibrated with the Ca²⁺ indicator for at least 10 min prior to the calcium measurements. Meanwhile, a baseline for EPSPs (0.05 Hz, 5–10 min) was established, and then b-APs were evoked by current injections into the soma or by antidromic stimulation in the alveus. Usually we evoked a train of b-APs (4–5, at 25–50 Hz) because the calcium signals from single b-APs were very small and sometimes even undetectable in the distal dendritic regions. The changes in $[Ca^{2+}]_i$ induced by the b-APs were measured in the soma and in the dendrites up to 300 μm from the soma. LTP was then induced using the TBP protocol, and fluorescence measurements were performed at the same regions of the dendrite. The results from one such experiment (Fig. 3a–d) show an increase in the Ca²⁺ signals associated with a train of b-APs in the distal region 15 min after induction of LTP (Fig. 3b). The increase was largest in the two small oblique dendrites (obl 1 and 2) close to the stimulating electrode and decreased with distance from the presumed site of LTP induction (Fig. 3b,c). In contrast to the distal dendritic region, almost no changes in the Ca²⁺ signals occurred at the soma and the proximal dendrite. Accordingly, the induction of LTP did not alter the size or shape of somatic APs, but

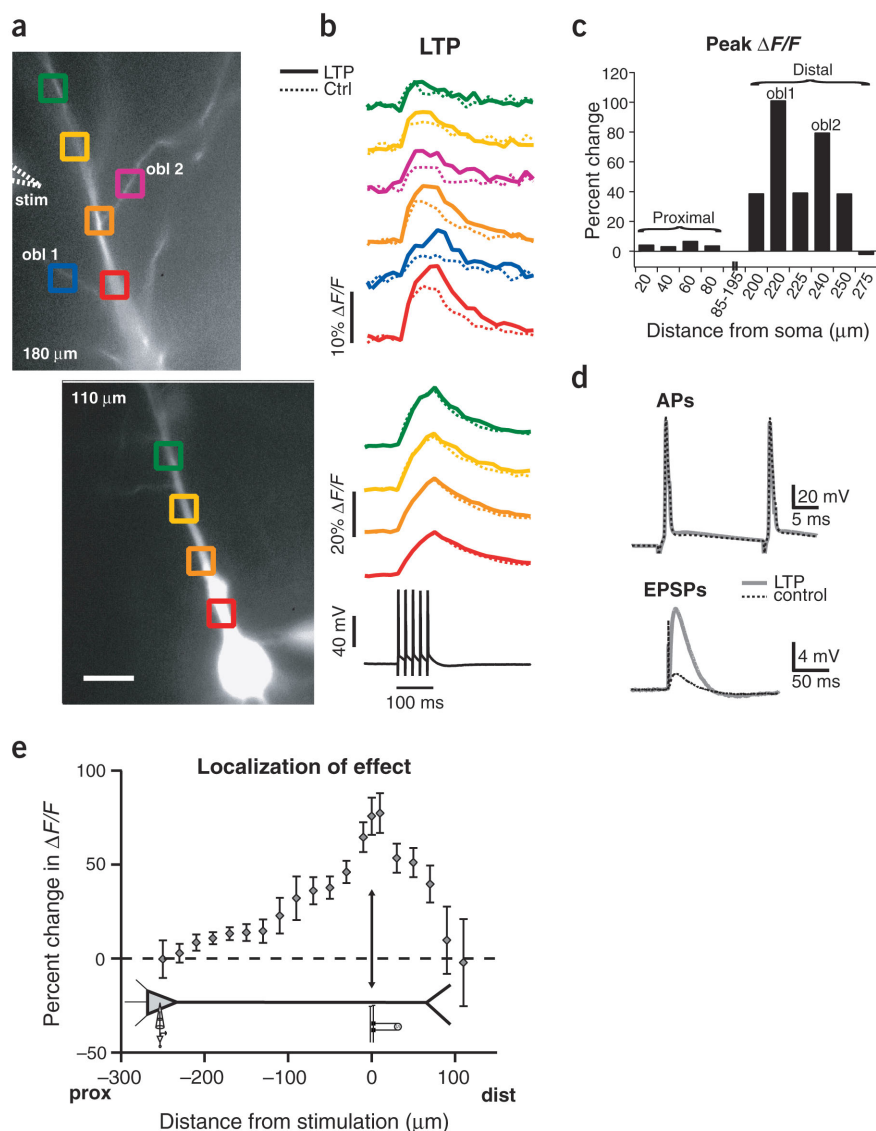


Figure 3 Increase in dendritic Ca^{2+} signals from b-APs after LTP induction. **(a)** Fluorescence image of the main apical dendrite with several oblique dendrites (for example, obl 1 + 2) of a CA1 pyramidal neuron. The position of the stimulating electrode is shown on the left close to the distal dendrite, and b-APs were evoked with current injections via a somatic recording pipette. Scale bar, 20 μm . **(b)** Changes in $[\text{Ca}^{2+}]_i$ (top traces) in response to a train of five b-APs at 50 Hz (lower trace) were measured as $\% \Delta F/F$ along the apical trunk and two oblique dendrites. The Ca^{2+} signals are shown before (dotted lines, ctrl) and after LTP induction (solid lines, LTP). The color of the traces corresponds to the colored boxes in **a**. Induction of LTP led to an increase in the Ca^{2+} signals from the b-APs in the distal but not the proximal part of the dendrite. In this case, the strongest changes occurred in the two oblique dendrites. **(c)** Changes in $[\text{Ca}^{2+}]_i$ (peak values) from b-APs after LTP are plotted as a function of distance from the soma. **(d)** LTP induction did not affect the APs at the soma, indicating that the increase in the Ca^{2+} signals was due to local changes in the dendrite. LTP induction elicited a strong, persistent increase in synaptic strength (EPSPs). **(e)** The Ca^{2+} signals from b-APs after LTP induction are normalized to control and plotted as percent change against the distance from the site of synaptic stimulation.

number of imaging trials to a minimum; it was therefore not feasible to describe the time course of the changes on a more detailed time scale. The results from these imaging experiments suggest that LTP induction is accompanied by a localized and persistent boost in the b-AP-evoked Ca^{2+} signals.

Changes in amplitude of b-APs after LTP

We also explored possible changes in the amplitude of b-APs by performing dendritic recordings near the presumed site of LTP induction. This method has the advantage of directly measuring the changes in b-AP amplitude, as opposed to the indirect approach permitted by Ca^{2+} imaging. However, the disadvantage is that if the changes in dendritic excitability are more or less confined to the dendritic region where LTP has occurred, then the recording must be performed at this specific region of the dendrite.

Nonetheless, dendritic whole-cell recordings were performed at a distance of $\sim 260 \mu\text{m}$ (same experiments as in Fig. 1e–h) from the soma, and b-APs were evoked by antidromic stimulation in the alveus (Figs. 4–6). The extracellular stimulation electrode used to evoke EPSPs was placed opposite to the recording electrode and LTP induced using the TBP protocol. The stimulus intensity was set to stimulate a larger number of Schaffer collaterals with the idea that this would improve our chances of recording at the appropriate dendritic sites; baseline EPSPs in the dendrites were in the range of 4 and 9 mV. There was no obvious change in the resting membrane potential as a result of LTP induction, but if necessary, this parameter was kept constant via current injection to exclude any effect of voltage on the amplitude of b-APs. A typical example of the results of these experiments is shown in Figure 4a. In this dendritic recording (270 μm from the soma),

strongly increased the synaptic strength (Fig. 3d). These results indicate that the boost of the b-APs and the associated Ca^{2+} signals occurred in the more distal dendritic tree near the site of the potentiated synapses.

What are the localization, magnitude, and time course of these changes? The first two parameters were addressed by plotting the changes in peak $\Delta F/F$ as a function of distance from the site of stimulation in the dendrite (Fig. 3e). At this presumed site of LTP, the increase in the Ca^{2+} signals was approximately 75% ($n = 15$). Outside this dendritic region, the amplification decreased in both the proximal and distal directions until it approached control values. This decline appeared to be somewhat steeper toward the distal dendrite, but because of limitations in the imaging method, we re-examined this issue with a more direct approach (see below). In contrast to changes seen at the site of potentiation, induction of LTP in the distal dendritic field changed the Ca^{2+} signals in the soma or the first 50–100 μm of the apical trunk by less than 10%. The increase in the Ca^{2+} signals was typically observed at about 10 min after LTP induction and persisted for the duration of the experiment (up to 60 min after TBP). To minimize phototoxicity and bleaching of the Ca^{2+} indicator, we kept the

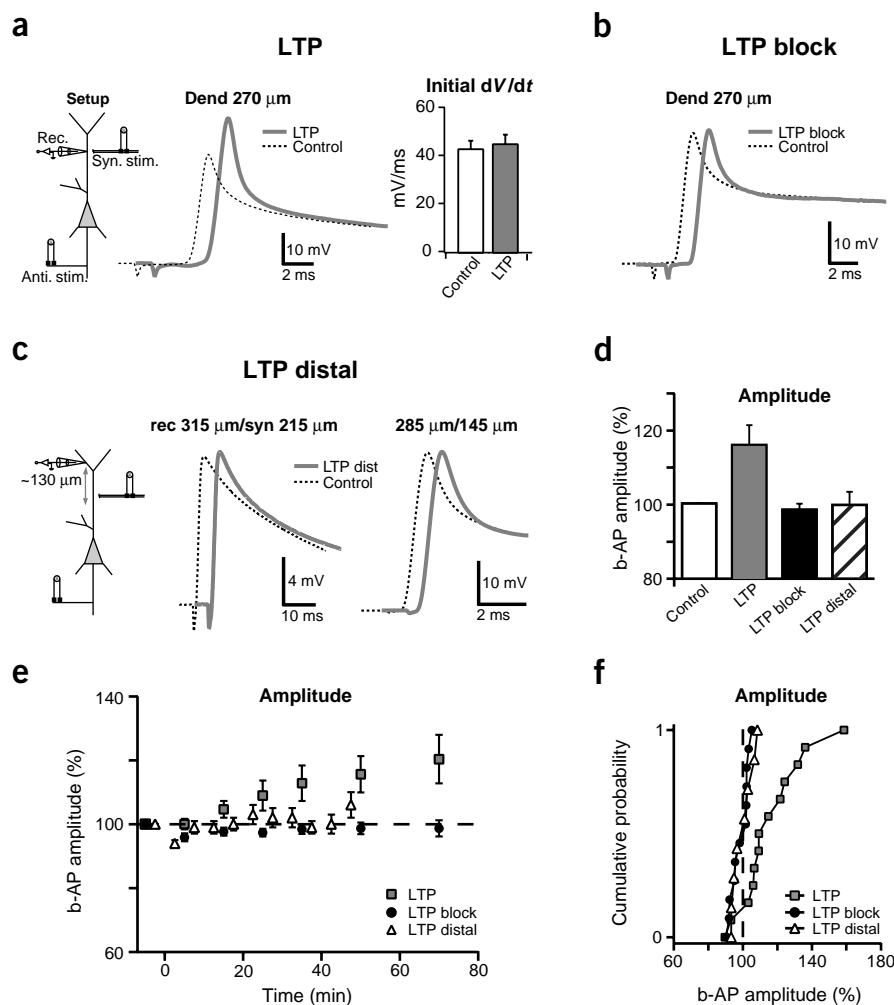


Figure 4 LTP was accompanied by an increase in dendritic b-AP amplitude. **(a)** LTP: diagram of the stimulating and recording configuration. Example of a dendritic whole-cell recording 270 μm from the soma showing a b-AP before and 50 min after induction of LTP. TBP increased the amplitude of the b-AP by 33%. Right, grouped data show no significant difference in the initial rate of rise of the b-APs in control and after induction of LTP, suggesting no change in the activation of Na⁺ channels under these conditions. **(b)** LTP block: block of LTP prevented increase in b-AP amplitude. Example of b-APs measured in the dendrite 270 μm from the soma before and after TBP in the presence of NMDA receptor antagonists (50 μM D,L-APV + 10 μM MK-801). **(c)** LTP distal: increase in b-AP amplitude was spatially localized. Diagram shows the position of the dendritic recording pipette, which was approximately 100–150 μm more distal than the presumed site of potentiation. The amplitude of the b-APs was unchanged at the distal recording site, suggesting that the increase was localized to the region of the potentiated pathway. **(d)** Summary plot of the changes in b-AP amplitude under different conditions. **(e)** Time course and magnitude of the change in b-AP amplitude for the different conditions. **(f)** Cumulative probability plot summarizes the data from **d**. Each point represents the magnitude of change relative to baseline for a given experiment, typically 40–45 min after TBP.

synaptic LTP was accompanied by a substantial 30% increase in the amplitude of the b-AP (from 35 mV to 46 mV, 50 min after TBP). Such a boost in the b-AP amplitude was consistently found in 13 dendrites; it averaged ~20% ($116 \pm 5\%$, $P < 0.01$; Fig. 4d–f) and accompanied an ~170% increase in the slope of the EPSPs (Fig. 1g).

Previous studies have shown that b-APs are dependent on voltage-gated Na⁺ channels within the apical dendrites of CA1 pyramidal neurons^{6,7,12}. Any modulation of these channels could therefore affect b-APs. If a change in the activation of the Na⁺ current is responsible for the increase in b-AP amplitude, then the initial rate of rise of the AP would increase as well, as it is primarily dependent on Na⁺ channel activation^{31,32}. Analysis of ten experiments revealed no significant difference in the initial dV/dt before and after LTP induction, suggesting that the increase in amplitude was not due to an increase in Na⁺ current (Fig. 4a). Additional control experiments were performed to assess whether the amplitude and the initial slope of the b-APs were influenced by an underlying depolarization from synaptic responses; however, adding the glutamate receptor antagonists CNQX (10–30 μM) and D,L-APV (50 μM) to the bath solution had no effect on the b-APs (amplitude $98 \pm 1\%$, initial slope $98 \pm 2\%$, $n = 6$, data not shown).

LTP block prevents changes in b-APs

Because LTP typically requires the activation of NMDA receptors, we tested whether inhibitors of NMDA receptors reduced the amplification of the b-AP by repeating the above experiments in the presence

of antagonists of the NMDA receptor (50 μM D,L-APV + 10 μM MK-801) (Fig. 4b,d–f). As expected, LTP induction was prevented or strongly reduced (EPSP slope, 146%; compare to Fig. 1f–h). Consistent with our hypothesis, the amplitude of b-APs did not change when compared with control ($98 \pm 2\%$, $n = 12$, $P = 0.3$).

The magnitude and time course of the changes in b-AP amplitude after LTP or in the presence of NMDA receptor antagonists are summarized in Figure 4d–f. Interestingly, during the first 5 min following LTP induction, the b-AP amplitude was usually slightly smaller compared to baseline, but then gradually increased over the next 40–50 min. At 40–50 min after LTP induction, the normalized amplitude of b-APs was approximately 20% larger than and significantly different from that for the drug-treated slices ($116 \pm 5\%$, $n = 13$ vs. $98 \pm 2\%$, $n = 12$, $P < 0.005$) or control.

Localization of changes in b-AP amplitude

How spatially restricted is the increase in b-AP amplitude? Does the boosted b-AP propagate more efficiently toward the very distal part of the dendrite, or does the amplitude decrease back to pre-LTP levels once the b-AP leaves the potentiated dendritic region? We addressed these questions by performing two sets of experiments. As described above, we used Ca²⁺ imaging to show that the increase in the Ca²⁺ signal from b-APs accompanying LTP induction is somewhat localized with respect to the site of synaptic input (Fig. 3e). Unfortunately, this method was not sensitive enough to detect Ca²⁺ signals from the very small b-APs in the distal regions of the dendrite. We therefore used a more direct and complementary approach by recording at dendritic sites close to stratum lacunosum-moleculare (296 ± 17 μm from soma, $n = 10$) and distal with respect to the potentiated pathway

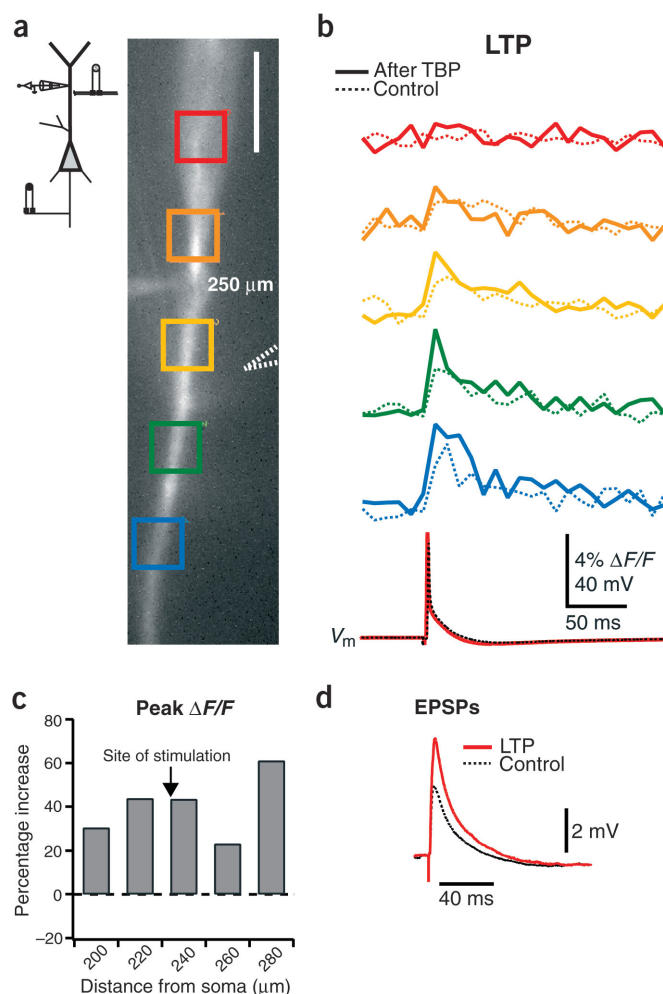


Figure 5 Distal dendritic b-APs and Ca^{2+} signals—LTP. **(a)** Fluorescence image of the main apical dendrite with a dendritic recording pipette and a stimulating electrode at a distance of 250 and 230 μm , respectively, from the soma (see also schematic). Scale bar, 20 μm . **(b)** Changes in $[\text{Ca}^{2+}]_i$ (top traces) in response to a single b-AP (lower trace) elicited by antidromic stimulation before (dotted lines, control) and after TBP (solid lines). The color of the traces corresponds to the colored boxes in **a**. Induction of LTP enhanced the amplitude of the b-AP and the associated Ca^{2+} signals in the dendrite. **(c)** The increases in $[\text{Ca}^{2+}]_i$ from the b-AP following LTP are plotted as a function of distance from the soma. **(d)** EPSPs were strongly potentiated following application of the TBP protocol.

(168 \pm 24 μm from the soma). LTP was induced as described above (EPSP slope, 181 \pm 20%, $n = 10$) and antidromically evoked b-APs were measured before and for 45 min following LTP induction. The results from two of those experiments are shown in **Figure 4c** and the summary for eight experiments is plotted in **Figure 4d–f**. LTP induction at a more proximal location did not affect the amplitude of b-APs recorded at the more distal site (24.6 \pm 3.0 mV vs. 24.6 \pm 3.2 mV, n.s., **Fig. 4d**). These results are in accordance with our Ca^{2+} imaging measurements and suggest that the amplification of b-APs does not extend far beyond the region of potentiation.

Changes in b-APs and associated Ca^{2+} signals

We next combined dendritic recordings and Ca^{2+} imaging to test whether LTP induction leads to an increase in the amplitude of b-APs

and produces an increase in Ca^{2+} signals from the same cell ($n = 4$). Single b-APs (**Fig. 5b**, lower traces) were recorded in the dendrite 250 μm from the soma and the associated Ca^{2+} signals (**Fig. 5b**, upper traces) were measured between 200 and 280 μm from the soma (**Fig. 5a,b**). The amplitude of the b-APs increased by approximately 5 mV following LTP induction (**Fig. 5d**). Accordingly, the Ca^{2+} influx from these b-APs was boosted as well. **Figure 5c** summarizes the changes in Ca^{2+} signals, plotted as a function of distance from the soma.

We repeated these experiments in the presence of NMDA receptor antagonists (50 μM D,L-APV + 10 μM MK-801; $n = 2$) to test whether the observed changes depended on LTP induction (**Fig. 6**). The b-APs (lower traces) were recorded at a distance of 225 μm from the soma, and the changes in the Ca^{2+} signals (upper traces) from these b-APs were measured in this and neighboring dendritic regions (**Fig. 6a,b**). Blocking LTP induction prevented any changes in the amplitude of b-APs, the associated Ca^{2+} signals in the dendrite (**Fig. 6c**) and the synaptic strength (**Fig. 6d**), suggesting that the measured modifications of dendritic function are coupled to synaptic plasticity.

Shift in I_A inactivation with LTP

What are the mechanisms underlying these localized changes in the dendrites that accompany synapse-specific LTP? We used cell-attached patch-clamp recordings from the distal dendrites of CA1 pyramidal neurons to test for changes in the properties of I_A , before and after LTP induction. These experiments were conducted under conditions comparable to the ones described thus far, that is, at near-physiological temperatures (33–34 $^{\circ}\text{C}$) and at dendritic distances of \sim 250 μm . The time course of the recordings was limited to about 25–35 min (including 15–20 min after LTP induction) due to limits in the longevity of patch recordings at these temperatures.

Subthreshold synaptic stimulation induced an initial current transient that resembled the first derivative of the membrane voltage (dV/dt , **Fig. 7a**); the integration of these current traces produced waveforms that approximate the shape of EPSPs³³ (**Fig. 7b**), and these waveforms were used to calculate changes in the slope of the response after LTP. Application of the TBP protocol resulted in strong LTP of the synaptic input, as seen clearly in the current traces or after integration of the current (slope of integral, 240 \pm 25%, $n = 23$, 10 min after TBP, **Fig. 7a–c**).

Voltage steps from -95 to $+55$ mV revealed an outward current composed of two distinct components, a transient—rapidly activating and inactivating—component (I_A) and a sustained component⁹. The outward current evoked by these steps peaked in <1 ms and was on average 29 \pm 21 pA at a distance of 259 \pm 22 μm from the soma ($n = 36$, see **Fig. 8a** for representative traces).

We measured either activation or inactivation properties of I_A using different voltage protocols in control conditions and then repeated these measurements 10–20 min after LTP induction using the same dendrite patches. In the first set of patches, we found that the voltage-range of inactivation for I_A was shifted approximately 6 mV in the hyperpolarized direction following the induction of LTP ($V_{1/2} = -69.2 \pm 2.4$ mV post LTP vs. -63.5 ± 1.7 mV control, $n = 9$, $P = 0.02$; see Methods and **Fig. 8a–c**). In another set of patches we found that, in contrast to inactivation, the I_A voltage-range of activation was unaltered ($V_{1/2} = +6.5$ mV post LTP vs. $+3.0$ mV control, n.s.; **Fig. 8c**). These alterations in the steady-state properties of dendritic I_A mean that the number of channels available for activation at rest (roughly -65 mV) was reduced by \sim 50% with LTP in these neurons (**Fig. 8d**). Finally we found that these changes in inactivation were blocked by NMDA receptor antagonists (50 μM D,L-APV and 10

μM MK-801, slope of synaptic input, $138 \pm 26\%$, $n = 5$, n.s.; $V_{1/2} = -63.4 \pm 0.6$ mV LTP block vs. -64.4 ± 0.5 mV control, $n = 5$, n.s.; Fig. 8e). Also, the changes in inactivation observed were not the result of any channel rundown or patch life-time dependence as time controls showed no difference in steady-state inactivation ($V_{1/2} = -64.9 \pm 1.2$ mV rundown vs. -64.7 ± 0.7 control, $n = 8$, n.s.; see Methods and Fig. 8f).

DISCUSSION

The principal conclusion from our results is that the induction of LTP can lead to specific, local and persistent changes in dendritic function—a form of intrinsic plasticity that accompanies synaptic plasticity. The net result of these activity-dependent changes is an increase in the excitability at, or near, the site of potentiation. These changes were mediated by a down-regulation of dendritic outward current and expressed as an increase in the amplitude of back-propagating action potentials and the associated Ca^{2+} influx. We present the following evidence to suggest an activity-dependent, localized increase in dendritic excitability: (i) enhancement of Ca^{2+} signals from b-APs within the dendritic region where the synapses were potentiated; (ii) amplification of b-APs in the same dendritic region; (iii) enhancement in both the amplitude of the b-APs and their associated Ca^{2+} signals decreased with distance from the region receiving synaptic input; and (iv) the steady-state inactivation range of A-type K^+ channels was shifted toward more hyperpolarized potentials at the presumed site of LTP. This shift markedly reduced the availability of outward current, particularly at voltages around the resting membrane potential. And finally (v), the changes in the b-AP amplitude and associated Ca^{2+} signals, as well as in the A-type K^+ current, were dependent on LTP induction.

It should be noted that the localization of the increase in dendritic excitability, as measured using Ca^{2+} imaging (Fig. 3e) and dendritic recordings (Fig. 4c), is likely to be an underestimate because of the distributed nature of the stimulated fibers. Moreover, evidence for clusters of A-type K^+ channels in spines³⁴ (A. Jeromin, A.F. & D.J., unpublished data) points to a role of these channels in signal integration at the level of individual synapses. The vast majority of synaptic input is received onto small dendritic branches called radial oblique branches in CA1 pyramidal neurons. These relatively short ($\sim 100 \mu\text{m}$), thin branches would provide a further degree of localization for the changes in membrane excitability observed here.

The most plausible explanation for our results is that dendritic A-type K^+ channels have a higher probability of being in an inactivated state during the expression phase of LTP, presumably due to the activation of one or more signal transduction pathways. This down-regulation of K^+ current would then be manifested as an enhancement of the amplitude of APs as they back-propagate through this dendritic region. In addition, there would be an increase in the amplitude of incoming synaptic activity and a decrease in threshold for locally generated APs^{9,10,14}.

A-type K^+ channels are important regulators of signal integration and propagation in the dendrites of hippocampal CA1 pyramidal neu-

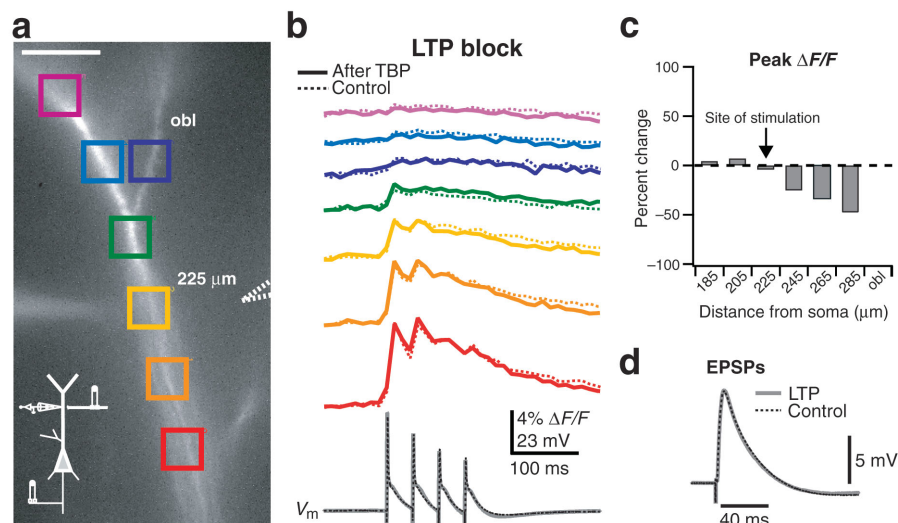


Figure 6 Distal dendritic b-APs and Ca^{2+} signals—LTP block. **(a)** Fluorescence image of an apical dendrite with a dendritic recording pipette and a stimulating electrode at a distance of $225 \mu\text{m}$ from the soma (see also schematic). Scale bar, $20 \mu\text{m}$. **(b)** Changes in $[\text{Ca}^{2+}]_i$ (top traces) in response to a train of four b-APs at 25 Hz (lower traces) elicited by antidromic stimulation were measured before (dotted lines, control) and after TBP in the presence of antagonists of the NMDA receptor (solid lines). The color of the traces corresponds to the colored boxes in **a**. In the presence of antagonists ($50 \mu\text{M}$ D,L-APV + $10 \mu\text{M}$ MK-801) no changes were induced in the amplitude of b-APs or in the Ca^{2+} signals in the dendrite. **(c)** The changes in $[\text{Ca}^{2+}]_i$ from the b-AP, 40 min after TBP, are plotted as a function of distance from the soma. **(d)** Potentiation of the EPSPs was blocked in the presence of NMDA receptor antagonists.

rons⁹. Their impact on dendritic signaling is profound and varied—the efficiency of action potential back-propagation, the capacity to generate dendritic Ca^{2+} plateau potentials, the shaping of EPSP amplitude and duration, and the threshold for local dendritic spike initiation are all influenced to some extent by the availability of dendritic A-type K^+ channels^{7,9,10,14,16,27}. Thus, dendritic A-type K^+ channels present a prime target for the regulation of dendritic function by the various signaling cascades produced by LTP-inducing stimulation.

Indeed, it has been shown that A-type K^+ channels can be regulated through direct phosphorylation (by PKA, PKC, CaMKII, MAPK) or through other mechanisms such as those mediated by arachidonic acid,

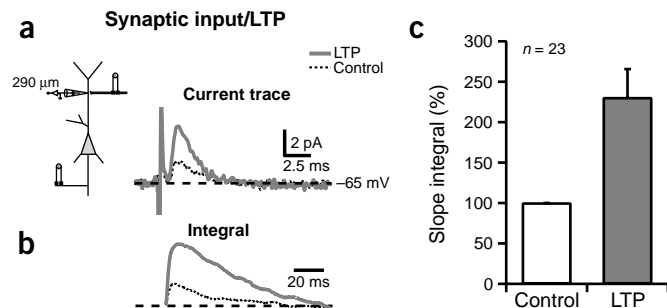


Figure 7 Dendrite-attached patch recordings revealed an increase in synaptic input with LTP. Synaptic input from Schaffer collateral stimulation before (control) and after induction of LTP (LTP) recorded in dendrite-attached configuration. **(a)** Current traces in response to subthreshold synaptic stimulation, demonstrating an increase in the capacitive current transients evoked by synaptic inputs following LTP induction. **(b)** Integral of current traces in **a**. **(c)** Analysis of 23 patches shows a strong increase in the slope of the integrals from synaptic inputs with LTP.

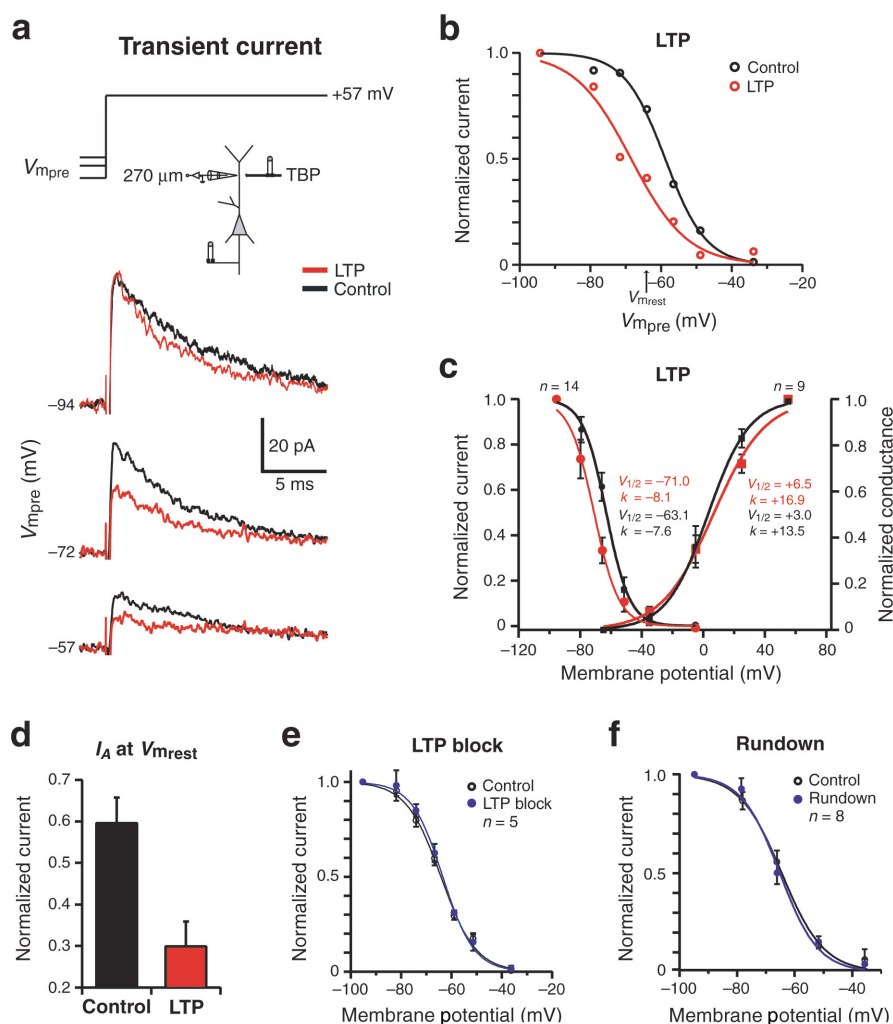


Figure 8 Hyperpolarized shift in steady-state inactivation of distal dendritic I_A with LTP. **(a)** Selected traces for the outward current evoked by step depolarizations from three different holding potentials to +57 mV in control and following LTP induction; dendrite-attached patch at a distance of 270 μm from the soma. After LTP induction (red traces), the size of the peak current evoked by these voltage steps decreased due to an increase in steady-state inactivation of dendritic I_A . Notably, there was no rundown of the current. Records have capacitive currents subtracted by scaling traces at smaller voltage amplitude (see Methods). **(b)** Steady-state inactivation of I_A before and after LTP induction in the same cell. The normalized current is plotted against the holding potential. **(c)** Group data showing activation ($n = 9$) and inactivation ($n = 14$) curves for I_A in the same distal dendritic patches before and after LTP induction. LTP shifted the inactivation curve by -7 mV with no change in their slopes, whereas there was no significant shift in the activation curve. **(d)** The hyperpolarized shift in the inactivation curve accompanying LTP resulted in an $\sim 50\%$ reduction in the number of channels available to be activated by a voltage step from the resting membrane potential to +55 mV. **(e)** LTP block using the NMDA receptor antagonists MK-801 (10 μM) and D,L-APV (50 μM) prevented the hyperpolarized shift of the inactivation curve. **(f)** Rundown of the peak amplitude of I_A did not cause the shift in the inactivation curve.

redox state and intracellular Ca^{2+} . In addition, auxiliary subunits can bind to these channels, and these subunits are potential targets for modulation (for review, see ref. 18). LTP induction and expression involves a number of signaling pathways, including the activation of protein kinases and the production of arachidonic acid. In CA1 pyramidal neurons, phosphorylation of A-type K^+ channels by PKA, PKC and MAPK has been shown to downregulate these channels by shifting the activation curve of I_A ^{8,14} rather than affecting the steady-state inactivation as found here. Arachidonic acid has been shown to reduce I_A and

to shift its inactivation to more hyperpolarized potentials^{10,15} and to increase the peak of b-APs^{8,14,16}. The effect of arachidonic acid on the inactivation of I_A would be consistent with the hyperpolarized shift in inactivation reported here. There are certainly other potential mechanisms, however, and further studies will be needed to examine the regulation of voltage-dependent conductances and neuronal excitability by intracellular signaling pathways.

Voltage-gated Na^+ channels are possible candidates for an activity-dependent modification of dendritic function, and several signaling pathways have been found to modulate this current^{14,17,35,36}. We have, however, provided evidence that the change in the amplitude of b-APs is not caused by either the recruitment of or a change in the properties of Na^+ channels. Such an additional contribution would result in an increase in the initial rate of rise of the b-AP because this parameter reflects the fast activation of these channels^{31,32}. It has been shown that Na^+ channels in the distal dendrites can enter a state of prolonged inactivation during a train of action potentials and that the activation of PKC can hasten the recovery from this inactivation. Changes in slow inactivation would also have been expected to change the rate of rise of the b-AP³⁷.

Other possible candidates for the modulation of a neuron's intrinsic electrical properties are voltage-gated Ca^{2+} channels²⁵. In the present study, we showed that the boosted b-AP amplitude was associated with an increased Ca^{2+} signal. Certainly some modulation of Ca^{2+} channels may have occurred with LTP and such a modulation could play a role, along with the increased b-AP amplitude, in the observed increase in dendritic Ca^{2+} signals. However, while the properties of dendritic Ca^{2+} channels make them good sensors of increases in b-AP amplitude^{4,5,12}, their currents are in general too slow and too small to make a substantial contribution to the b-AP amplitude³⁸. We thus favor the hypothesis that the non-synaptic plasticity in dendritic excitability results primarily from changes in A-type K^+ channel activity, but we do not rule out additional and concomitant changes in the properties of other dendritic channels.

Other conductances could also be modulated following the induction of synaptic plasticity. A recent study²⁴ reported that the induction of LTP and LTD induces bidirectional changes involving the hyperpolarization-activated cation current I_h and NMDA receptors, thereby increasing or decreasing the linearity of spatial summation of synaptic inputs. Although these authors observed no change in I_A following LTP induction, a few important methodological differences between these two studies need to be highlighted. First, there is a dif-

ference in the LTP induction protocol: synaptic stimulation at 20 Hz for 0.5 s, ten times at 4-s intervals versus the theta-burst pairing protocol used here. Second, their study used somatic recordings, whereas we used distal dendritic recordings to assess local changes in signaling and channel properties more directly. Finally, differences in the age of the animals (14–22 days old versus 6–10 weeks in our study) or temperature of the experiment (28–29 °C versus 33–36 °C in our experiments) might play a role.

These studies suggest that the efficiency by which action potentials propagate into the dendritic arbor is influenced by the prior activity of the neuron^{39,40}. This is an important concept because b-APs have many critical functions in CA1 pyramidal neurons^{1–3}. b-APs are important in the induction of both LTP and LTD, and an improvement in back-propagation should lower the threshold for further synaptic plasticity in the dendritic regions affected^{12,13,41,42}. The net effect here is a type of positive feedback for all forms of synaptic plasticity. In addition, b-APs are involved in the induction of dendritic Ca²⁺ plateau potentials that are effective triggers of action potential bursts in these cells^{27,38}. The likelihood of burst firing could therefore be increased in neurons that have undergone some level of LTP. Finally, the Ca²⁺ influx associated with b-APs and Ca²⁺ plateaus could potentially be involved in all of the signaling events ascribed to intracellular Ca²⁺ including ion channel modulation, neurotransmitter receptor cycling, dendritic and spine growth and mobility.

Furthermore, by acting as a braking influence on the subthreshold activation of dendritic ion channels that carry inward current, dendritic A-type K⁺ channels are important players in shaping the integrative properties of the dendrites^{9,10,27}. Any reduction in the availability of dendritic A-type K⁺ channels will increase the impact of Na⁺ and Ca²⁺ channel activation on the integration of EPSPs, reducing the level of synchrony and spatial clustering required for supra-linear summation of those inputs. In the end, the impact of the synaptic input would be elevated and the type of computation performed by the dendrite altered^{43,44}. E-S potentiation²⁰, for example, has been explained based on either alterations in GABAergic inhibition^{45–47} or a modulation of intrinsic conductances in the postsynaptic membrane^{24,48–50}. Local increases in dendritic excitability, such as those reported here (see also ref. 24), could contribute to an enhanced propagation of EPSPs toward the site of action potential initiation.

Together these data suggest that specific input patterns to the dendritic arbors of CA1 pyramidal neurons could set up regional changes in dendritic excitability. That is, the dendritic branches receiving synaptic input properly timed with action potential output would experience not only an increase in the efficacy of synaptic transmission but also a long-lasting increase in branch excitability. Thus, the next time a neuron receives the same input pattern, the impact of that input will be elevated by an enhanced amount of supra-linear summation, an increased incidence of burst firing and a higher propensity for further synaptic plasticity. In this way, these highly non-linear and compartmentalized modifications could improve the storage and processing capabilities of hippocampal neurons and circuits^{30,43,44}.

METHODS

Electrophysiology. Hippocampal slices (350 μm) were prepared from adult (6–10 week-old) male Sprague Dawley rats using standard procedures⁹. Neurons were visualized with differential interference contrast (DIC) microscopy using a Zeiss Axioskop II microscope (Oberkochen), fitted with a 60× (Olympus) water-immersion objective. Recordings were made at 33–36 °C. The extracellular recording solution contained 125 mM NaCl,

2.5 mM KCl, 1.25 mM NaH₂PO₄, 25 mM NaHCO₃, 2.0 mM CaCl₂, 1.0 mM MgCl₂ and 25 mM dextrose, and was bubbled with 95% O₂/5% CO₂ (pH 7.4). The whole-cell recording pipette solution contained 120 mM potassium gluconate, 20 mM KCl, 10 mM HEPES, 0.2 mM EGTA, 2 mM MgCl₂, 4 mM NaATP, 0.3 mM Tris GTP, 14 mM phosphocreatine and 0.05–0.1 mM bis-fura-2 (pH 7.3 with KOH). Biocytin (0.5%) was included in the internal solution in some experiments for later morphological analysis. Recorded neurons had resting potentials between –61 and –72 mV, and were kept at a constant membrane potential during the course of the experiment.

Drugs applied in the bath were made from aqueous stock solutions (D,L-APV, MK-801, CNQX, bicuculline methiodide, picrotoxin). All drugs were obtained from Sigma. Experiments were performed with addition to the bath of bicuculline methiodide (10 μM) and picrotoxin (10 μM) to block GABA_A receptor-mediated responses. Area CA3 was removed from the slice to diminish repetitive firing resulting from reduced GABAergic inhibition.

Whole-cell patch-clamp recordings made from the somata and/or the dendrites of CA1 pyramidal neurons using an Axon Instruments Axoclamp 2A or a Dagan BVC-700. Signals were filtered at 3 kHz and sampled at 10–50 kHz. EPSPs were elicited by extracellular stimulation using a bipolar tungsten electrode positioned in stratum radiatum close (within 25 μm) to the dendrite of the recorded neuron at a distance of 200–300 μm from the soma. The initial rate of rise of the b-APs was usually calculated between 5 and 10 mV above the resting membrane potential.

For cell-attached recordings, the pipette solution consisted of 125 mM NaCl, 10 mM HEPES, 2.5 mM KCl, 1 mM CaCl₂, 1 mM MgCl₂ and 1.0 μM TTX (pH 7.4 with NaOH). Pipettes were pulled from borosilicate glass and the tips were fire-polished (6–9 MΩ). To reduce the capacitance, the pipettes were wrapped in parafilm. Cell-attached recordings, using an Axopatch 1C amplifier (Axon Instruments) were analog-filtered at 2 kHz and sampled at 10–50 kHz. Linear leakage and capacitive currents were digitally subtracted by scaling traces at smaller command voltages, where no voltage-dependent current was activated. The peak current amplitude of the transient component was calculated by subtracting the sustained component; the sustained component was measured as the mean values of the last 50 ms of the current trace. For activation plots, chord conductance ($E_K = 104$ mV, calculated from Nernst equation), calculated from the peak ensemble current amplitude from a holding potential of –30 mV relative to the resting membrane potential (V_{rest}), was normalized to maximum and plotted as a function of step potential (from V_{rest} to +120 mV relative to V_{rest}). V_{rest} was measured at the end of the experiment by breaking through the membrane, and this potential was then used to calculate values of voltage command. Steady-state inactivation was studied using depolarizing test pulses to a fixed voltage (+120 mV) preceded by a series of pre-pulse conditioning potentials ranging from –30 to +30 mV (all relative to V_{rest}). Curves are sigmoidal fits of the data to single Boltzmann functions (Igor Pro, Wavemetrics). The effect of rundown on inactivation properties of I_A was measured by determining inactivation plots before and after rundown of the current; rundown was produced by repetitive voltage steps from –30 to +120 mV relative to V_{rest} until the maximum current was reduced by ~20%. For activation and inactivation plots, statistics were calculated only from those cells from which a reasonable fit was obtained. The resting membrane potential was -65.2 ± 0.6 (n = 29).

Group data are expressed as mean ± s.e.m unless otherwise stated. Statistical significance was calculated using paired or unpaired *t*-tests.

Fluorescence imaging. Methods for Ca²⁺ fluorescence imaging were similar to those described previously⁷. A Photometrix Quantix:57 CCD camera (Photometrics) with a 535 × 512 pixel array and single wavelength (380 nm) excitation was used to quantify changes in [Ca²⁺]_i by calculating $\Delta F/F$.

ACKNOWLEDGMENTS

We wish to acknowledge L. Schexnayder for early work on this project at Baylor and thank H. Miyakawa and M. Inoue for help with the project at the MBL. In addition, we thank X. Chen, R. Gray, M. Haque, M. Migliore, R. Chitwood, N. Poolos, A. Jeromin and M. Ginger for important contributions. Supported by grants from the National Institute of Neurological Disorders and Stroke (NINDS) and the National Institute of Mental Health (NIMH) (D.J. & J.M.), the Human Frontier Science Program (D.J.) and the Alexander von Humboldt Foundation (A.F.).

COMPETING INTERESTS STATEMENT

The authors declare that they have no competing financial interests.

Received 16 October; accepted 16 December 2003

Published online at <http://www.nature.com/natureneuroscience/>

- Yuste, R. & Tank, D.W. Dendritic integration in mammalian neurons, a century after Cajal. *Neuron* **16**, 701–716 (1996).
- Johnston, D., Magee, J.C., Colbert, C.M. & Christie, B.R. Active properties of neuronal dendrites. *Annu. Rev. Neurosci.* **19**, 165–186 (1996).
- Stuart, G., Spruston, N., Sakmann, B. & Häusser, M. Action potential initiation and backpropagation in neurons of the mammalian CNS. *Trends Neurosci.* **20**, 125–131 (1997).
- Jaffe, D.B. *et al.* The spread of Na⁺ spikes determines the pattern of dendritic Ca²⁺ entry into hippocampal neurons. *Nature* **357**, 244–246 (1992).
- Miyakawa, H. *et al.* Synaptically activated increases in Ca²⁺ concentration in hippocampal CA1 pyramidal cells are primarily due to voltage-gated Ca²⁺ channels. *Neuron* **9**, 1163–1173 (1992).
- Spruston, N., Schiller, Y., Stuart, G. & Sakmann, B. Activity-dependent action potential invasion and calcium influx into hippocampal CA1 dendrites. *Science* **268**, 297–300 (1995).
- Frick, A., Magee, J., Koester, H.J., Migliore, M. & Johnston, D. Normalization of Ca²⁺ signals by small oblique dendrites of CA1 pyramidal neurons. *J. Neurosci.* **23**, 3243–3250 (2003).
- Yuan, L.L., Adams, J.P., Swank, M., Sweatt, J.D. & Johnston, D. Protein kinase modulation of dendritic K⁺ channels in hippocampus involves a mitogen-activated protein kinase pathway. *J. Neurosci.* **22**, 4860–4868 (2002).
- Hoffman, D.A., Magee, J.C., Colbert, C.M. & Johnston, D. K⁺ channel regulation of signal propagation in dendrites of hippocampal pyramidal neurons. *Nature* **387**, 869–875 (1997).
- Ramakers, G.M. & Storm, J.F. A postsynaptic transient K⁺ current modulated by arachidonic acid regulates synaptic integration and threshold for LTP induction in hippocampal pyramidal cells. *Proc. Natl. Acad. Sci. USA* **99**, 10144–10149 (2002).
- Johnston, D. *et al.* Active dendrites, potassium channels and synaptic plasticity. *Philos. Trans. R. Soc. Lond. B Biol. Sci.* **358**, 667–674 (2003).
- Magee, J.C. & Johnston, D. A synaptically controlled, associative signal for Hebbian plasticity in hippocampal neurons. *Science* **275**, 209–213 (1997).
- Watanabe, S., Hoffman, D.A., Migliore, M. & Johnston, D. Dendritic K⁺ channels contribute to spike-timing dependent long-term potentiation in hippocampal pyramidal neurons. *Proc. Natl. Acad. Sci. USA* **99**, 8366–8371 (2002).
- Johnston, D., Hoffman, D.A., Colbert, C.M. & Magee, J.C. Regulation of back-propagating action potentials in hippocampal neurons. *Curr. Opin. Neurobiol.* **9**, 288–292 (1999).
- Müller, W. & Bittner, K. Differential oxidative modulation of voltage-dependent K⁺ currents in rat hippocampal neurons. *J. Neurophysiol.* **87**, 2990–2995 (2002).
- Colbert, C.M. & Pan, E. Arachidonic acid reciprocally alters the availability of transient and sustained dendritic K⁺ channels in hippocampal CA1 pyramidal neurons. *J. Neurosci.* **19**, 8163–8171 (1999).
- Tsubokawa, H. & Ross, W.N. Muscarinic modulation of spike backpropagation in the apical dendrites of hippocampal CA1 pyramidal neurons. *J. Neurosci.* **17**, 5782–5791 (1997).
- Schrader, L.A., Anderson, A.E., Varga, A.W., Levy, M. & Sweatt, J.D. The other half of Hebb: K⁺ channels and the regulation of neuronal excitability in the hippocampus. *Mol. Neurobiol.* **25**, 51–66 (2002).
- Bliss, T.V. & Collingridge, G.L. A synaptic model of memory: long-term potentiation in the hippocampus. *Nature* **361**, 31–39 (1993).
- Bliss, T.V. & Gardner-Medwin, A.R. Long-lasting potentiation of synaptic transmission in the dentate area of the unanaesthetized rabbit following stimulation of the perforant path. *J. Physiol.* **232**, 357–374 (1973).
- Alkon, D.L., Lederhendler, I. & Shoukimas, J.J. Primary changes of membrane currents during retention of associative learning. *Science* **215**, 693–695 (1982).
- Turrigiano, G., Abbott, L.F. & Marder, E. Activity-dependent changes in the intrinsic properties of cultured neurons. *Science* **264**, 974–977 (1994).
- Aizenman, C.D. & Linden, D.J. Rapid, synaptically driven increases in the intrinsic excitability of cerebellar deep nuclear neurons. *Nat. Neurosci.* **3**, 109–111 (2000).
- Wang, Z., Xu, N.L., Wu, C.P., Duan, S. & Poo, M.M. Bidirectional changes in spatial dendritic integration accompanying long-term synaptic modifications. *Neuron* **37**, 463–472 (2003).
- Yasuda, R., Sabatini, B.L. & Svoboda, K. Plasticity of calcium channels in dendritic spines. *Nat. Neurosci.* **6**, 948–955 (2003).
- Magee, J.C. Voltage-gated ion channels in dendrites. In *Dendrites* (eds. Stuart, G., Spruston, N. & Häusser, M.) 139–160 (Oxford Univ. Press, Oxford, UK, 1999).
- Reyes, A. Influence of dendritic conductances on the input-output properties of neurons. *Annu. Rev. Neurosci.* **24**, 653–675 (2001).
- Hoffman, D.A., Sprengel, R. & Sakmann, B. Molecular dissection of hippocampal theta-burst pairing potentiation. *Proc. Natl. Acad. Sci. USA* **99**, 7740–7745 (2002).
- Christie, B.R., Eliot, L.S., Ito, K., Miyakawa, H. & Johnston, D. Different Ca²⁺ channels in soma and dendrites of hippocampal pyramidal neurons mediate spike-induced Ca²⁺ influx. *J. Neurophysiol.* **73**, 2553–2557 (1995).
- Golding, N.L., Staff, N.P. & Spruston, N. Dendritic spikes as a mechanism for cooperative long-term potentiation. *Nature* **418**, 326–331 (2002).
- Hodgkin, A.L. & Katz, B. The effect of sodium ions on the electrical activity of the giant axon of the squid. *J. Physiol. (Lond.)* **108**, 37–77 (1949).
- Colbert, C.M., Magee, J.C., Hoffman, D.A. & Johnston, D. Slow recovery from inactivation of Na⁺ channels underlies the activity-dependent attenuation of dendritic action potentials in hippocampal CA1 pyramidal neurons. *J. Neurosci.* **17**, 6512–6521 (1997).
- Magee, J.C. & Johnston, D. Synaptic activation of voltage-gated channels in the dendrites of hippocampal pyramidal neurons. *Science* **268**, 301–304 (1995).
- Alonso, G. & Widmer, H. Clustering of KV4.2 potassium channels in postsynaptic membrane of rat supraoptic neurons: an ultrastructural study. *Neuroscience* **77**, 617–621 (1997).
- Gasparini, S. & Magee, J.C. Phosphorylation-dependent differences in the activation properties of distal and proximal dendritic Na⁺ channels in rat CA1 hippocampal neurons. *J. Physiol.* **541**, 665–672 (2002).
- Cantrell, A.R. & Catterall, W.A. Neuromodulation of Na⁺ channels: an unexpected form of cellular plasticity. *Nat. Rev. Neurosci.* **2**, 397–407 (2001).
- Colbert, C.M. & Johnston, D. Protein kinase C activation decreases activity-dependent attenuation of dendritic Na⁺ current in hippocampal CA1 pyramidal neurons. *J. Neurophysiol.* **79**, 491–495 (1998).
- Magee, J.C. & Carruth, M. Dendritic voltage-gated ion channels regulate the action potential firing mode of hippocampal CA1 pyramidal neurons. *J. Neurophysiol.* **82**, 1895–1901 (1999).
- Tsubokawa, H., Offermanns, S., Simon, M. & Kano, M. Calcium-dependent persistent facilitation of spike backpropagation in the CA1 pyramidal neurons. *J. Neurosci.* **20**, 4878–4884 (2000).
- Quirk, M.C., Blum, K.I. & Wilson, M.A. Experience-dependent changes in extracellular spike amplitude may reflect regulation of dendritic action potential back-propagation in rat hippocampal pyramidal cells. *J. Neurosci.* **21**, 240–248 (2001).
- Markram, H., Lübke, J., Frotscher, M. & Sakmann, B. Regulation of synaptic efficacy by coincidence of postsynaptic APs and EPSPs. *Science* **275**, 213–215 (1997).
- Linden, D.J. The return of the spike: postsynaptic action potentials and the induction of LTP and LTD. *Neuron* **22**, 661–666 (1999).
- Poirazi, P. & Mel, B.W. Impact of active dendrites and structural plasticity on the memory capacity of neural tissue. *Neuron* **29**, 779–796 (2001).
- Poirazi, P., Brannon, T. & Mel, B.W. Pyramidal neuron as two-layer neural network. *Neuron* **37**, 989–999 (2003).
- Abraham, W.C., Gustafsson, B. & Wigstrom, H. Long-term potentiation involves enhanced synaptic excitation relative to synaptic inhibition in guinea-pig hippocampus. *J. Physiol.* **394**, 367–380 (1987).
- Lu, Y.M., Mansuy, I.M., Kandel, E.R. & Roder, J. Calcineurin-mediated LTD of GABAergic inhibition underlies the increased excitability of CA1 neurons associated with LTP. *Neuron* **26**, 197–205 (2000).
- Staff, N.P. & Spruston, N. Intracellular correlate of EPSP-spike potentiation in CA1 pyramidal neurons is controlled by GABAergic modulation. *Hippocampus* **13**, 801–805 (2003).
- Taube, J.S. & Schwartzkroin, P.A. Mechanisms of long-term potentiation: EPSP/spike dissociation, intradendritic recordings, and glutamate sensitivity. *J. Neurosci.* **8**, 1632–1644 (1988).
- Chavez-Noriega, L.E., Halliwell, J.V. & Bliss, T.V. A decrease in firing threshold observed after induction of the EPSP-spike (E-S) component of long-term potentiation in rat hippocampal slices. *Exp. Brain Res.* **79**, 633–641 (1990).
- Jester, J.M., Campbell, L.W. & Sejnowski, T.J. Associative EPSP-spike potentiation induced by pairing orthodromic and antidromic stimulation in rat hippocampal slices. *J. Physiol.* **484**, 689–705 (1995).